J|A|C|S COMMUNICATIONS

Published on Web 02/03/2010

# Selective Growth of Monoclinic and Tetragonal Zirconia Nanocrystals

Kazuyoshi Sato,* Hiroya Abe, and Satoshi Ohara

*Joining and Welding Research Institute, Osaka University, 11-1 Mihogaoka, Ibaraki, Osaka 567-0047 Japan*

Received December 19, 2009; E-mail: k-sato@jwri.osaka-u.ac.jp

In this communication, we demonstrate for the first time a selective growth of single-crystalline pure monoclinic and tetragonal $ZrO_2$ nanocrystals of <10 nm diameter, driven by controlling their surface energy. The growth of metal oxide nanocrystals with a well-organized crystalline phase is of fundamental and technological interest because in this way it is possible to tune their size-dependent unique properties,[1,2] and thus establish their potential application in chemistry, electronics, optics, magnetics, and mechanics. $ZrO_2$ is a case in point, with a phase-dependent potential application in a number of technologies. Monoclinic $ZrO_2$ is important for catalysis,[3] gate dielectrics,[4] and bioactive coatings on bone implants,[5] while tetragonal and cubic $ZrO_2$ are promising candidates for fuel cell electrolytes,[6] oxygen sensors,[7] and phase-transformation-toughened structural materials.[8]

In particular, the growth of pure monoclinic $ZrO_2$ nanocrystals of <10 nm diameter is a challenging task in the selective growth of the different phases, since a high-temperature tetragonal phase is stable at room temperature as the consequence of the dominance of the surface energy contribution to the Gibbs free energy of formation in this size range.[9] A report by Zhang et al. suggests that the surface energy of oxides can be controlled by capping the surface with an organic substance.[10] They successfully grow the unstable (001) faceted $CeO_2$ by capping with decanoic acid. Although surface capping-assisted growth using similar anionic substances was also applied to $ZrO_2$, the resulting nanocrystals of <10 nm diameter still chiefly exhibited a tetragonal phase.[11,12] Herein, we report the facile selective growth route of pure monoclinic and tetragonal $ZrO_2$ nanocrystals of <10 nm diameter, with and without a cationic capping agent, $N(CH_3)_4^+$.

In a typical procedure, a $Zr^{4+}$ precursor ($ZrOCl_2 \cdot 8H_2O$, 0.01 mol) was dissolved in a basic aqueous solution (pH $\approx$ 10.5) containing a mixture of either $N(CH_3)_4HCO_3$ (tetramethyl-ammonium hydrogen carbonate; TMAHC)/$N(CH_3)_4OH$ (tetramethyl-ammonium hydroxide; TMAH) or $KHCO_3$/KOH. The clear solution of dissolved precursor was transferred into a 50 mL, Teflon-lined, stainless steel autoclave and heat treated at 150 °C. The products were obtained as well-dispersed colloidal solutions. $ZrO_2$ nanocrystals in the solution were purified by washing ten times with deionized water using ultrafiltration, with a molecular weight cutoff of 3000 for subsequent characterizations. The yield of $ZrO_2$ nanocrystals was almost 100% in both TMAHC/TMAH and $KHCO_3$/KOH systems. The $ZrO_2$ nanocrystals were characterized by transmission electron microscopy (TEM; JEOL JEM-2100F) with an accelerating voltage of 200 kV, X-ray diffraction (XRD; JEOL JDX-3530M) with Cu K$\alpha$ radiation ($\lambda$ = 0.154178 nm) at 40 kV and 40 mA, Raman spectroscopy (Horiba Jobin Yvon LabRAM ARAMIS) at room temperature with 532 nm excitation line of an diode-pumped solid state laser, and UV−vis adsorption spectroscopy (Shimadzu, UV-2450) with a double-beam recording spectrometer using 1 cm quartz cells.

Figure 1 shows TEM images of $ZrO_2$ nanocrystals grown in the TMAHC/TMAH and $KHCO_3$/KOH systems. These images clearly

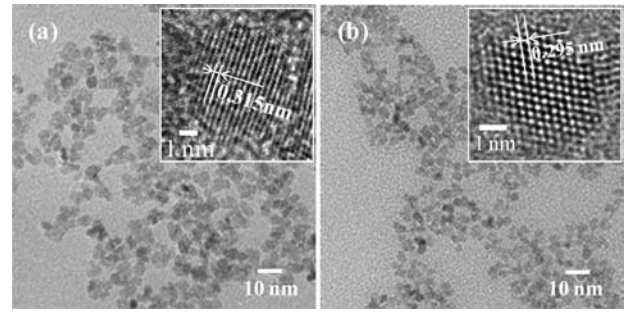


***Figure 1.*** TEM images of $ZrO_2$ nanocrystals grown in the (a) TMAHC/TMAH and the (b) $KHCO_3$/KOH systems. Each respective inset shows an HRTEM image of an isolated nanocrystal.

indicate that both nanocrystals consist entirely of crystals of a uniform size of <10 nm diameter. The inset shows the high-resolution TEM (HRTEM) image of an isolated nanocrystal, indicating the single-crystalline nature of the nanocrystals grown in both systems. The lattice spacing is 0.315 and 0.295 nm, corresponding to (−111) of monoclinic and (111) of tetragonal $ZrO_2$ for the nanocrystals grown in the TMAHC/TMAH and the $KHCO_3$/KOH systems, respectively. Figure S-1 (Supporting Information) shows the size distribution of the $ZrO_2$ nanocrystals in the aqueous solution measured by dynamic light-scattering method, showing the nanocrystals almost perfectly dispersed in the aqueous solution by taking into account that the hydrodynamic diameter overestimates by several nanometers the real size.[13]

The XRD patterns of the powdered nanocrystals shown in Figure 2 further confirm that the respective phases observed in the HRTEM images represent the entire nanocrystals in both systems. The peaks are relatively broad, supporting the very small crystalline size. The sizes estimated by Scherrer's formula using full width of half maxima of (−111) for monoclinic and (111) for tetragonal phases were almost the same at 5.4 and 5.2 nm, respectively. The inset of Figure 2 shows the Raman spectra recorded for colloidal solutions of $ZrO_2$ nanocrystals. For the nanocrystals grown in the TMAHC/TMAH system, the purely monoclinic structure is confirmed by the observation of 13 Raman modes of the 18 ($9A_{1g} + 9B_{1g}$) expected by symmetry analysis,[14] which provides evidence that the growth of monoclinic $ZrO_2$ nanocrystals shown above was driven by the surface capping with $N(CH_3)_4^+$ (denoted as $TMA^+$ in the following text), and not by the surface energy reduction through agglomeration by drying. The broad Raman band for the tetragonal $ZrO_2$ nanocrystals indicates that they involve highly disordered lattice defects.[14]

Optical absorption spectra of the colloidal $ZrO_2$ solutions shown in Figure 3 provide information relating to the lattice defects. Two absorption shoulders are clearly observed at around 5.2 and 5.7 eV for the $ZrO_2$ nanocrystals grown in the TMAHC/TMAH system. These are almost identical to the optical band gaps of bulk monoclinic $ZrO_2$,[15] indicating less defective lattices.[16] The tetrago-



10.1021/ja910712r 

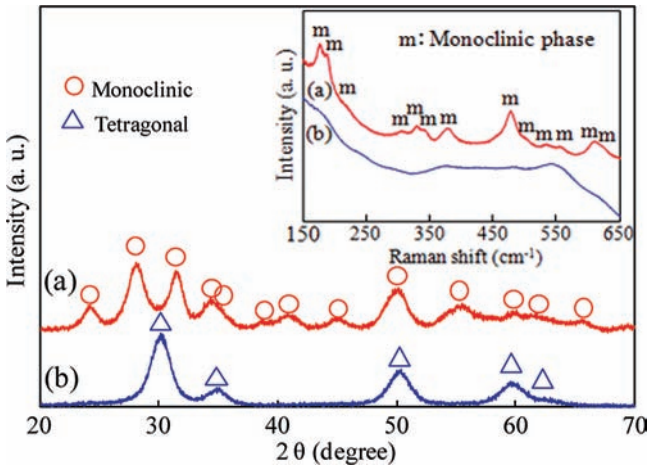


***Figure 2.*** XRD profiles of $ZrO_2$ nanocrystals grown in the (a) TMAHC/TMAH and the (b) $KHCO_3$/KOH systems. The inset shows Raman spectra of colloidal solutions of $ZrO_2$ nanocrystals grown in the (a) TMAHC/TMAH and the (b) $KHCO_3$/KOH systems.

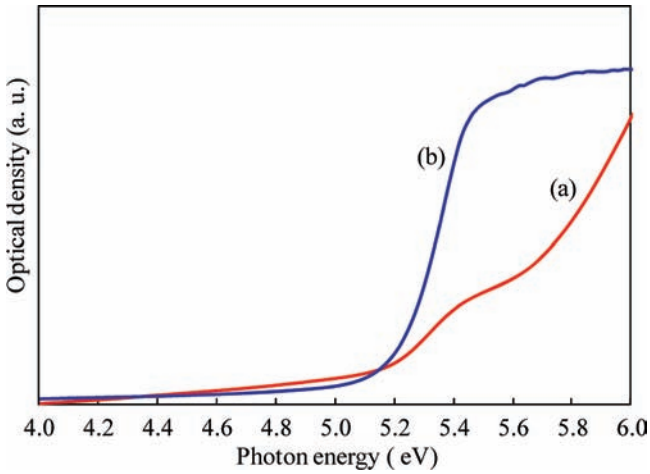


***Figure 3.*** Optical absorption spectra of colloidal solutions of $ZrO_2$ nanocrystals grown in the (a) TMAHC/TMAH and the (b) $KHCO_3$/KOH systems.

nal $ZrO_2$ showed only one absorption shoulder at a lower photon energy (approximately at 5.1 eV) than those of monoclinic $ZrO_2$, indicating the presence of many lattice defects, probably cation impurity and/or oxygen vacancy.[14] Inductively coupled plasma-atomic emission spectroscopy revealed that the concentration of $K^+$ in the tetragonal $ZrO_2$ was negligible ($<10^{-7}$ mol·g$^{-1}$). Thus, it can be concluded that the major lattice defects in the tetragonal $ZrO_2$ are oxygen vacancies, which is consistent with a previous report.[16]

Here we discuss how the selective growth of monoclinic and tetragonal $ZrO_2$ nanocrystals was achieved. Monoclinic $ZrO_2$ nanocrystals may be formed due to the reduction of surface energy through capping with $TMA^+$, since the capping with organic substances has the potential to reduce the surface energy of oxides by more than 1.7 J·m$^{-2}$ compared with bare surface as suggested by the literature,[10,17,18] while the surface energy of monoclinic $ZrO_2$ is only approximately 0.4 J·m$^{-2}$ higher than that of tetragonal.[9] The differential thermal analysis (DTA, Figure S-2 in Supporting Information) showed that $TMA^+$ persists on the nanocrystals up to 280 °C. The considerably higher temperature than the vaporization temperature of free TMAH (157 °C) indicates that $TMA^+$ successfully caps the surface of $ZrO_2$ nanocrystals. By contrast, the absence of $K^+$ in the $ZrO_2$ grown in the $KHCO_3$/KOH system as shown above indicates that the $K^+$ does not cap the nanocrystals; thereby, the tetragonal phase is spontaneously formed.[9]

It is suggested that the energy state of surface oxygen plays a vital role in the size-dependent phase stability of $ZrO_2$ nanocrystals, since the stable phase strongly depends on the sign of charge of the capping agent, i.e., monoclinic $ZrO_2$ is obtained when the negatively charged surface oxygen is capped with oppositely charged $TMA^+$. By contrast, the tetragonal phase is stabilized when the nanocrystals are capped with anionic substances,[11,12] in which the surface oxygen may be exposed to the surrounding medium the same as in the case of uncapped nanocrystals ($KHCO_3$/KOH system in this study). The oxygen vacancies in the tetragonal $ZrO_2$ may be formed as a consequence of relaxation of the unstable surface oxygen.

In summary, our study offers a simple approach for the selective growth of pure monoclinic and tetragonal $ZrO_2$ nanocrystals of <10 nm diameter capped with and without $TMA^+$, respectively. The present concept, surface energy control via the capping with an adequate agent, is a promising universal approach to control the crystal phase of technologically important oxide nanocrystals such as $Al_2O_3$, $TiO_2$, $BaTiO_3$, and $PbTiO_3$, consequently enabling us to tune their unique properties.

**Acknowledgment.** This work was supported by a Scientific Research Grant from the Ministry of Education, Science, Sports and Culture of Japan.

**Supporting Information Available:** Size distributions of colloidal $ZrO_2$ nanocrystals determined by DLS method (Figure S-1); DTA analysis data of $TMA^+$-capped $ZrO_2$ nanocrystals and TMAH pentahydrate (Figure S-2). This material is available free of charge via the Internet at http://pubs.acs.org.

## References

(1) Garcia-Barriocanal, J.; Rivera-Calzada, A.; Varela, M.; Sefrioui, Z.; Iborra, E.; Leon, E.; Pennycook, J.; Santamaria, J. *Science* **2008**, *321*, 676.
(2) Hoshina, T.; Wada, S.; Kuroiwa, Y.; Tsurumi, T. *Appl. Phys. Lett.* **2008**, *93*, 192914.
(3) He, D.; Ding, Y.; Luo, H.; Li, C. *J. Mol. Catal.* **2004**, *208*, 267.
(4) Wilk, G. D.; Wallace, R. M.; Anthony, J. M. *J. Appl. Phys.* **2001**, *89*, 5243.
(5) Wang G.; Meng F.; Ding C.; Chu P. K.; Liu X. *Acta Biomater.*; available online at Elsevier Sciencehttp://www.elsevier.com.
(6) Shin, J. H.; Chao, C.-C.; Huang, H.; Prinz, F. B. *Chem. Mater.* **2007**, *19*, 3850.
(7) León, C.; Lucia, M. L.; Santamaría, J. *Phys. Rev. B* **1997**, *55*, 882.
(8) Garvie, R. C.; Hannink, R. H.; Pascoe, R. T. *Nature* **1975**, *258*, 703.
(9) Garvie, R. C. *J. Phys. Chem.* **1978**, *82*, 218.
(10) Zhang, J.; Ohara, S.; Umetsu, M.; Naka, T.; Hatakeyama, Y.; Adschiri, T. *Adv. Mater.* **2007**, *19*, 203.
(11) Joo, J.; Yu, T.; Kim, Y. W.; Park, H. M.; Wu, F.; Zhang, J. Z.; Hyeon, T. *J. Am. Chem. Soc.* **2003**, *125*, 6553.
(12) Zhao, N.; Pan, D.; Nie, W.; Ji, X. *J. Am. Chem. Soc.* **2006**, *128*, 10118.
(13) Bootz, A.; Vogel, V.; Schubert, D.; Kreuter, J. *Eur. J. Pharm. Biopharm.* **2004**, *57*, 369.
(14) Michel, D.; Perez, M.; Jorba, Y.; Collongues, R. *J. Raman Spectrosc.* **1976**, *5*, 163.
(15) Kwok, C.- K.; Aita, C. R. *J. Appl. Phys.* **1989**, *66*, 2756.
(16) Yashima, M.; Tsunekawa, S. *Acta Crystallogr.* **2006**, *B62*, 161.
(17) Kaneko, K.; Inoke, K.; Freitag, B.; Hungria, A. B.; Midgley, P. A.; Hansen, T. W.; Zhang, J.; Ohara, S.; Adschiri, T. *Nano Lett.* **2007**, *7*, 421.
(18) Conesa, J. C. *Surf. Sci.* **1995**, *339*, 337.

JA910712R